

Dinuclear complexes of a pseudocalixarene macrocycle: structural consequences of intramolecular hydrogen bonding†

Julia Barreira Fontecha, Sandrine Goetz and Vickie McKee*

Chemistry Department, Loughborough University, Loughborough, UK LE11 3TU

Received 3rd September 2004, Accepted 17th November 2004

First published as an Advance Article on the web 1st February 2005

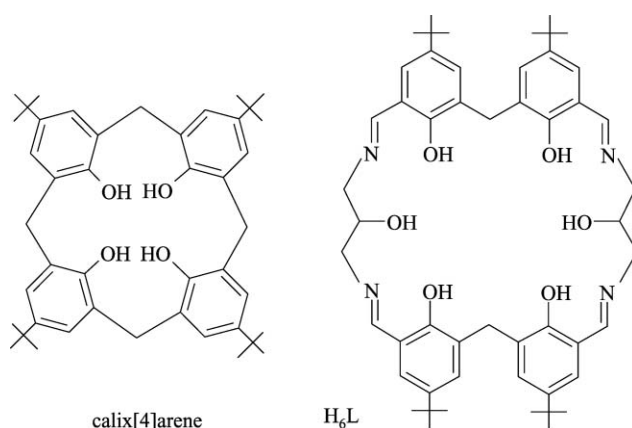
A series of dinuclear complexes of a pseudocalixarene macrocycle H_6L containing two 2,2'-methylenediphenol groups have been synthesised and structurally characterised. Using divalent metal ions, complexes containing a common hyperbolic paraboloid (saddle) $M_2(H_4L)^{2+}$ core are formed. The structure is controlled by two strong O–H–O interactions resulting from metal ion-promoted monodeprotonation of the methylenediphenol units. The metal ions are located in a cleft within which neutral or anionic guests can bind. Use of trivalent metal ions leads to complete deprotonation of the phenol groups and loss of the saddle conformation.

Introduction

Schiff-base ‘‘Robson-type’’ macrocycles containing potentially bridging phenol groups have been used to synthesise dinuclear homo- and heteronuclear systems for approximately 30 years. Detailed investigation of the chemistry of dinuclear^{1–4} and, more recently, polynuclear^{5–9} phenol-based macrocyclic complexes has permitted significant insights in a number of areas, including magnetochemistry, site selection, catalytic and bioinorganic model chemistry.

Phenol-based macrocyclic ligands show apparent similarities to the extensive family of calixarenes, and can be described as azacalixarenes.¹⁰ However, there are two important differences in coordination chemistry between calixarenes and Robson macrocycles. First, the inclusion in the macrocycles of relatively soft imine or amine nitrogen donors in addition to the phenolic oxygen atoms widens the range of metal ions that might be expected to bind with high stability constants. Indeed, typically the macrocyclic ligands readily complex transition metals while the calixarenes are chiefly viewed as hosts for hard metal ions. Second, the geometries of metal complexes formed are significantly different. The calixarenes are relatively rigid due to the methylene links around the ring and the (generally) small size of the cavity which mean that in genuine calixarenes a planar conformation is sterically prohibited. For this reason, coordinated metal ions cannot take advantage of the bridging potential of the phenol groups, and the complexes are generally mononuclear. In contrast, macrocyclic ligands can complex using some or all of their phenolic oxygen donors in the bridging mode and are usually di- or polynuclear. They are also often close to planar, although the more rigid tetraphenol examples are, to some extent, bowl-shaped.^{6,11–13}

In an attempt to combine some of the properties of the Schiff-base and calixarene systems we are developing a new range of Schiff-base pseudocalixarene macrocycles based on the dialdehyde precursor 2,2'-dihydroxy-5,5'-di-*tert*-butyl-3,3'-methanediyldibenzaldehyde (dhtmb, Scheme),^{14,15} a related macrocycle has also been reported by Hisaeda and co-workers.¹⁶ Unlike most aza- or oxo-calixarenes (in which inserts are made at each methylene link)^{10,17,18} the new ligands preserve two methylenediphenol units intact while inserting softer imine donors along with other potentially bridging donors between them. The ligands can be viewed as formally derived from



calix[4]arene by insertion of two diimine bridging sections (=N–R–N=) into the ring *i.e.* they are members of the family of expanded calixarenes.

In a recent communication¹⁵ we reported that the ligand H_6L , derived from condensation of dhtmb with 1,3-diaminopropan-2-ol, can form di- tri- and tetranuclear complexes with copper(II) ions. In this paper we describe the synthesis and characterisation of a set of dinuclear complexes of the same ligand. Emphasis is on the interplay of metal oxidation state with intramolecular hydrogen-bonding in defining an unusually rigid conformation in the complexes of divalent ions.

Results and discussion

The synthesis of the precursor 2,2'-dihydroxy-5,5'-di-*tert*-butyl-3,3'-methanediyldibenzyl alcohol from *p-tert*-butylphenol is well known in calixarene chemistry.¹⁹ It has been used both in the stepwise synthesis of calixarenes and, more recently, to form large homooxacalixarenes.¹⁷ This precursor can be oxidised to the dialdehyde dhtmb using manganese dioxide.^{14,20}

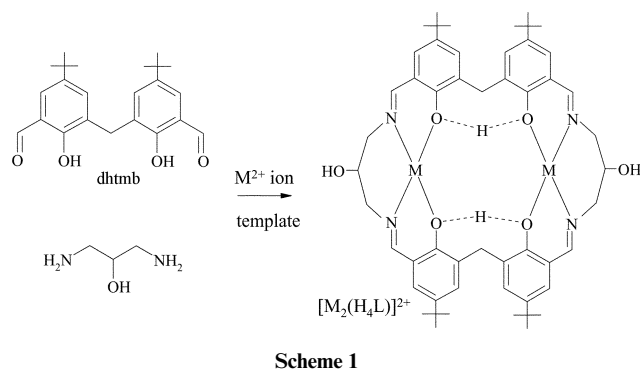
The complexes listed in Table 1 were prepared by standard template techniques as described in the experimental section and illustrated in Scheme 1. Successful formation of the macrocycle was confirmed initially by IR spectroscopy where formation of the Schiff-base was indicated by disappearance of the carbonyl (1658 cm^{-1} in dhtmb) and amine stretches along with appearance of an imine stretching band at *ca.* 1630 cm^{-1} for the $M(II)$ complexes, dropping to 1618 cm^{-1} in the dimanganese(III) complex (**8**). Further indication of the dinuclear nature of the complexes was obtained from mass spectral data (Table 1). Each of the divalent metal complexes shows a peak corresponding to a singly charged ion containing the dimetallic fragment $[M_2(H_3L)]^+$ (or $[M_2(H_4L)]^+$ in the case of complex **6**). In a

† Electronic supplementary information (ESI) available: Details of the synthesis of the complexes, superimposed structures (3 Figures), details of ¹H and ¹³C NMR assignments for complex **2**, and PDB files suitable for CHIME for each structure (7 separate files). See <http://www.rsc.org/suppdata/dt/b4/b413639j>

Table 1 Selected data for the complexes

Complex	Colour	FAB or ESI ^a mass spectral data (<i>m/z</i> , rel. intensity, assignment)
1 1a	Green	969, 100%, [Cu ₂ (H ₄ L) – H] ⁺
2 2a	Pale yellow	973, 50%, [Zn ₂ (H ₄ L) – H] ⁺ 1009, 100%, [Zn ₂ (H ₄ L)Cl] ⁺
3	Green	^a 479, 40%, [Ni ₂ (H ₄ L)] ²⁺ ^a 957, 100%, [Ni ₂ (H ₄ L) – H] ⁺ ^a 995, 10%, [Ni ₂ (H ₄ L)Cl] ⁺
4 4a	Yellow	959, 25%, [Co ₂ (H ₄ L) – H] ⁺ 995, 100%, [Co ₂ (H ₄ L)(H ₂ O) ₂ – H] ⁺
5 5a	Green	^a 479, 100%, [Ni ₂ (H ₄ L)] ²⁺ ^a 957, 50%, [Ni ₂ (H ₄ L) – H] ⁺ ^a 1059, 15% [Ni ₂ (H ₄ L)(ClO ₄)] ⁺
6 6a	Green	958, 100%, [Ni ₂ (H ₄ L)] ⁺
7 7a	Pale yellow	971, 100%, [Zn ₂ (H ₄ L) – H] ⁺
8 8a	Brown	951, 100%, [Mn ₂ (H ₂ L) + H] ⁺ 987, 20%, [Mn ₂ (H ₂ L)Cl + 2H] ⁺ 1119, 30%, [Mn ₂ (H ₂ L)Cl ₂ (dmsO)(H ₂ O)] ⁺

^a For ESI-MS relative abundance is given for cone voltage = 90 V.

**Scheme 1**

number of cases fragments including anions were also observed. Careful comparison of experimental and calculated isotope patterns shows that, in many cases, the complexes are reduced in the LSIMS experiment.

In general, the complexes were obtained from the reaction mixtures as powders and recrystallised from ethanol or dmf to obtain crystals suitable for X-ray studies. Frequently the recrystallisation resulted in a different set of solvate molecules (coordinated and/or in the lattice) but the basic M₂(H₄L)X unit (where X = bridging group) remained intact. Relevant geometric data for this unit with the range of metal ions and bridging groups investigated are summarised in Table 2. Interestingly,

if an ethanol solution of complex **7** (where M = Zn, and X = NO₃⁻), is exposed to air for several days the nitrate anions appear to be slowly replaced by a carbonate anion, yielding a complex analysing as Zn₂(H₄L)(CO₃)(H₂O)₄. This reaction suggests the possibility of activating guests bound to the metal ions and is under further investigation.

The structure of dicopper(II) complex **1a** has been communicated previously and the dizinc(II) complex **2a** is isomorphous with it; two views of the [Zn₂(H₄L)Cl]⁺ cation are shown in Fig. 1. The metal ions are each coordinated to two imine groups, two phenol oxygen atoms and a bridging chloride ion (M–Cl–M 104.55(5) and 104.80(14)^o for the copper and zinc complexes, respectively). The geometry at the metals is square pyramidal with the chloride ligand as the apical donor. The Jahn–Teller effect accounts for the observation that the Cu–Cl bonds are significantly longer than the Zn–Cl equivalents (Table 2). In the zinc complex (but not the copper analog), there is some disorder at the metal sites involving minor six-coordinate components (20% at Zn1 and 40% at Zn2). In the minor component the zinc ions lie in the plane of their macrocyclic donors and each has a water molecule as the sixth ligand.

The macrocycle adopts a saddle conformation (a hyperbolic paraboloid) with the basal planes about each metal ion inclined at ca. 86^o to each other (Table 2). This shape is maintained by two strong hydrogen bonds linking adjacent phenol oxygen atoms, O1–O2 and O4–O5, (Table 2). This structure is consistent with

Table 2 Selected structural parameters

Complex	M–X–M/ ^o	M–M/Å	M–X _{br} /Å	Interplanar angle/ ^o	O–H–O ^b /Å
1a	Cu–Cl–Cu	3.9998(12)	2.514(1), 2.542(1)	86.73(13)	2.414(4), 2.402(4)
2a	Zn–Cl–Zn	3.656(3) ^c	2.303(2), 2.311(2) ^c	86.03(8)	2.412(4), 2.406(4)
4a	Co–(H ₂ O)–Co	4.2123(16)	2.394(3)	83.01(10)	2.385(8), 2.398(7)
5a	Ni–(H ₂ O)–Ni	4.2176(11)	2.390(2)	81.39(7)	2.395(6), 2.397(6)
6a	Ni–(NO ₃)–Ni	4.6041(7)	2.085(4), 2.117(3)	77.30(7)	2.430(4), 2.440(4)
7a	Zn–(NO ₃)–Zn	4.4454(7)	2.344(8) ^c , 2.107(7) ^c	79.09(7)	2.480(3), 2.426(3)
8a	Mn–Mn ^d	7.6252(10)	– ^d	29.52(13)	5.068(4), 5.067(4) ^e

^a Angle between the planes of the (imine)₂(phenol)₂ donors at each metal ion. ^b Methylene-diphenol H-bond. ^c Involves some disordered atoms. ^d No bridge present. ^e No H-bond present.

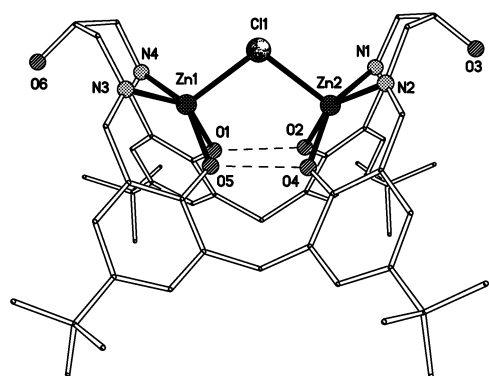
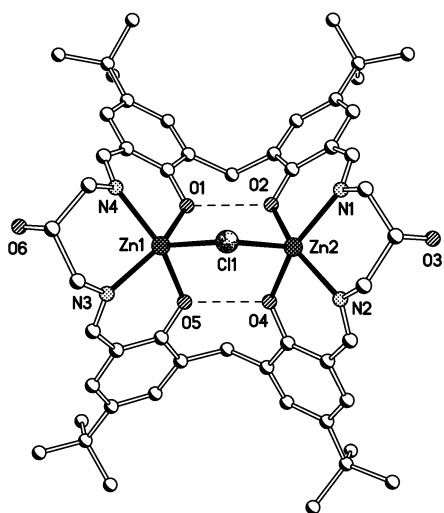


Fig. 1 Two views of the $[\text{Zn}_2(\text{H}_4\text{L})\text{Cl}]^+$ cation of **2a**. Hydrogen bonds are shown as dashed lines; hydrogen atoms and the minor components of disorder have been omitted for clarity.

loss of one proton from each methylenediphenol unit, resulting in a phenol–phenolate interaction. It is also in agreement with the stoichiometric data which suggest the macrocycle is doubly deprotonated. The pendant alcohol groups (O3 and O6) are not involved in bonding to the metal ions but they form hydrogen bonds to the non-coordinated chloride ion Cl2, forming one-dimensional chains through the lattice. The solvate ethanol molecule is also hydrogen-bonded to Cl2 but the ether solvate molecules are non-bonded and lie in channels between the cations.

The analogous nickel complex $[\text{Ni}_2(\text{H}_4\text{L})\text{Cl}]\text{Cl}\cdot 4\text{H}_2\text{O}$ (**3**) has been prepared but not crystallized. On the basis of analytical and mass spectral data it seems likely to contain the same chloro bridged structure, probably with water as sixth ligand to each nickel ion.

The dicobalt(II) and dinickel(II) complexes **4a** and **5a** constitute a second isomorphous pair; the structure of the $[\text{Co}_2(\text{H}_4\text{L})(\text{H}_2\text{O})(\text{EtOH})_2]^{2+}$ cation is shown in Fig. 2. In these cations the chloro bridge has been replaced by water and the metal ions are six-coordinate. The additional ethanol ligands lie within folds of the macrocycle and do not alter the overall shape of the macrocyclic cation, which is similar to the previous pair. As before, each 2,2'-methylene-diphenol unit is monodeprotonated and the phenols are linked by short hydrogen bonds (Table 2). The guest water molecule is hydrogen bonded to two ethanol molecules (O4–O(ethanol) distances 2.713(9) and 2.712(9) Å for **4a** and 2.705(8) and 2.718(7) Å for **5a**). Once again, hydrogen bonding involving the pendant alcohols, perchlorate anions, coordinated and lattice ethanol, links the cations into chains which run along the *b* axis.

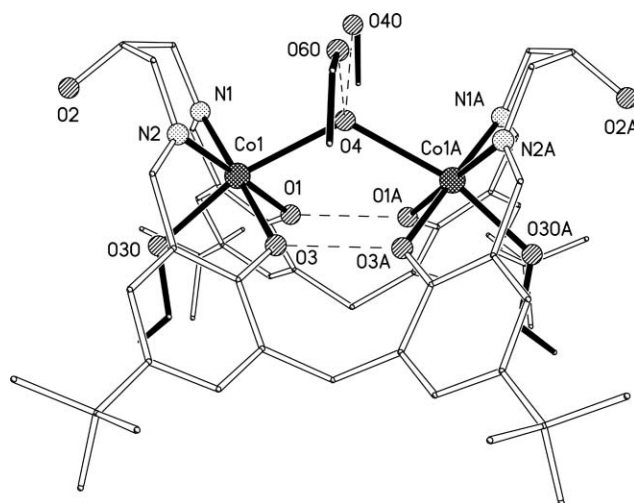


Fig. 2 The $[\text{Co}_2(\text{H}_4\text{L})(\text{H}_2\text{O})(\text{EtOH})_2]^{2+}\cdot 2\text{EtOH}$ cation of **4a** (isomorphous with the Ni(II) analog **5a**). Hydrogen bonds are shown as dashed lines; hydrogen atoms and the minor components of disorder have been omitted for clarity.

A search of the Cambridge Crystallographic Database^{21,22} shows a number of cobalt and nickel complexes with aqua bridges, most commonly where the metal–metal distance is controlled by other bridging groups (commonly carboxylates).²³ The mean M–OH₂ distances are 2.17 Å for cobalt(II) and 2.14 Å for nickel(II) and the ranges are 2.08–2.27 and 1.91–2.42 Å for cobalt and nickel complexes respectively. It is also noteworthy that the bridges with the longest Ni–OH₂ distances are unsymmetric with the second bond considerably shorter.^{24,25} In the present case, where the bridge has mirror symmetry, the M–OH₂ bonds are amongst the longest reported to date (2.39 Å, Table 2) and approximately 0.25 Å longer than the corresponding bonds to the coordinated ethanol molecules. Examination of Fig. 2 shows that the Co–OH₂ (or Ni–OH₂) bonds are not perpendicular to the planes of the macrocyclic donors but inclined at an angle of *ca.* 77° and that the M–O(H₂)–M angle has opened out to 123.3(3) and 123.9(2)° for the cobalt and nickel complexes, respectively. Taken together, these observations suggest that the water is weakly bonded within in the preformed cleft, where the Co–Co and Ni–Ni distances are restrained by the shape of the macrocycle.

The nitrate-bridged dinickel(II) and dizinc(II) complexes **6a** and **7a** constitute a third pair, again showing short hydrogen bonds across the monodeprotonated 2,2'-methylene-diphenol units (Table 2) and overall saddle conformation. These structures are not isomorphous. In $[\text{Ni}_2(\text{H}_4\text{L})(\text{NO}_3)(\text{dmf})_2]^+$ (Fig. 3) the nitrate acts as a *syn,anti*-1,3-bridge with the mean plane of the nitrate ion tilted at *ca.* 35° to the mean plane of Ni1, Ni2, O11 and O12. The nickel ions are six-coordinate (the sixth ligand being a dmf molecule in each case) and have quite regular geometry. The Ni–ONO₂ distances are unremarkable but the Ni–Ni distance is larger than for the aqua-bridged analog and the interplanar angle shows the cavity is a little more open (Table 2). In the dizinc(II) cation $[\text{Zn}_2(\text{H}_4\text{L})(\text{NO}_3)(\text{EtOH})]^+$ (Fig. 4) one of the metal ions is six-coordinate (with ethanol as the sixth ligand) and the other is five-coordinate. The bound nitrate ion is disordered 60:40 over two positions, the major one is bound in the same way as complex **6a**, but the minor component is monodentate, coordinated only to the five-coordinate zinc ion (Zn2). The cations are linked into chains by hydrogen bonding involving the pendant alcohols, the uncoordinated nitrate anion and the coordinated ethanol molecule.

The structure of the dimanganese(III) complex $[\text{Mn}_2(\text{H}_2\text{L})(\text{Cl})_2(\text{dmf})(\text{dmsO})]\cdot 1.5\text{dmf}\cdot 0.3\text{Et}_2\text{O}$ is very different from those discussed previously; two views of the neutral complex **8a** are shown in Fig. 5. The manganese ions are six-coordinate, each having chloride and a solvent molecule (dmf or dmsO) as the

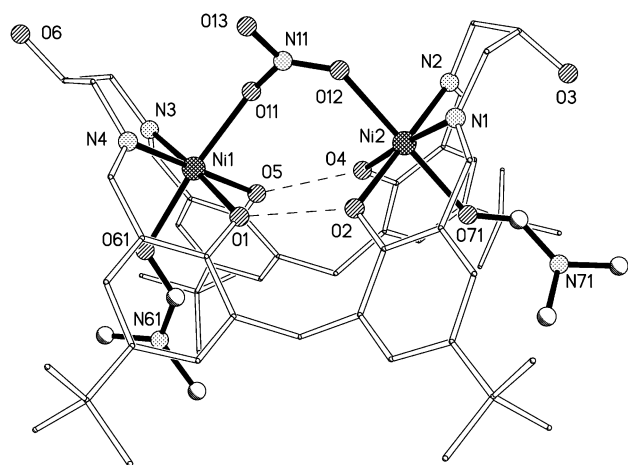


Fig. 3 The $[\text{Ni}_2(\text{H}_4\text{L})(\text{NO}_3)(\text{dmf})_2]^+$ cation of **6a**. Hydrogen bonds are shown as dashed lines; hydrogen atoms and the minor components of disorder have been omitted for clarity.

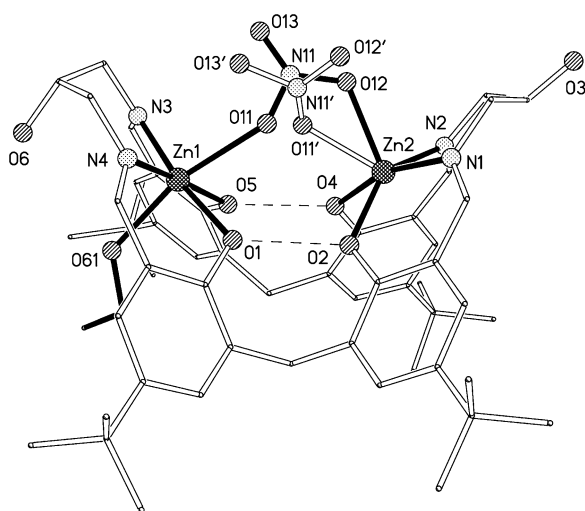


Fig. 4 The $[\text{Zn}_2(\text{H}_4\text{L})(\text{NO}_3)(\text{EtOH})]^+$ cation of **7a**. Hydrogen bonds are shown as dashed lines. Both components of the disordered nitrate ion are shown, the major component is that with black bonds.

non-macrocyclic ligands and each showing the expected Jahn–Teller extension. In contrast to the previous structures, the metal ions are well separated and there is no exogenous bridge linking them. The saddle-shape of the macrocycle has been lost and the phenolate groups in each methylenediphenolate are rotated with respect to one another so that one is tilted above the plane of the macrocycle and the other is tilted below (corresponding to the 1,2-alternate conformation in calix[4]arene terminology²⁶). As a consequence of this, the metal ions also lie one on each side of the macrocyclic plane. The resulting conformation is very similar to that of the related mononuclear manganese(III) Schiff base complex $[\text{Mn}(\text{salpn})\text{Cl}(\text{MeOH})]$,²⁷ suggesting the presence of the methylenediphenolate groups is not significant in determining the geometry in this case. Hydrogen bonding between one of the coordinated chloride ions and a pendant alcohol group (C11–O3 3.035(7) Å) links the molecules into zigzag chains.

The difference in conformation between complexes **1a–7a** and that of complex **8a** can be ascribed to the complete deprotonation of the 2,2'-methylene-diphenol groups in the dimanganese(III) complex. This, in turn, is due to the higher oxidation state of the Mn(III) ion; it is a better Lewis acid than the M(II) ions and effectively lowers the $\text{p}K_a$ of the coordinated phenols. In the absence of the intramolecular hydrogen bond the phenol oxygen atoms and the metal ions can move apart and the macrocyclic cleft opens out to a conformation very similar to that of simpler Schiff-base analogs.²⁷

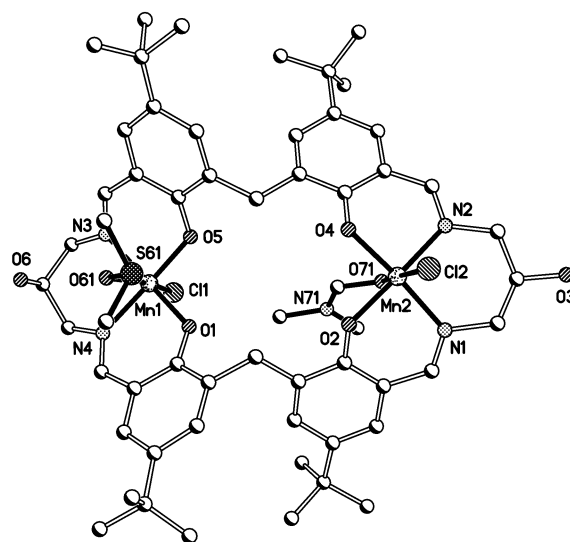


Fig. 5 Two views of the Mn(III) complex $[\text{Mn}_2(\text{H}_2\text{L})(\text{Cl})_2(\text{dmf})(\text{dmsO})]$ (**8a**).

The structures of the $\text{M}_2(\text{H}_4\text{L})$ skeletons of complexes **1a–7a** are almost superimposable; changing the non-macrocyclic ligands or even the coordination number of the metal ions has very little effect. This suggests that their conformation is controlled primarily by the two intramolecular phenol–phenolate hydrogen bonds and that the bridging ligand is simply occupying the preformed cleft resulting from the hydrogen-bonding. The phenol–phenolate interaction can be assigned to the (–)CAHB (negative charge-assisted hydrogen bonds) class,^{28,29} although the presence of the coordinated metal ions might be expected to moderate the charge. (–)CAHB interactions are normally strong hydrogen bonds with O–H–O in the range 2.38–2.5 Å and bond energies up to 31 kcal mol^{–1} and are probably best viewed as three-centre–four-electron covalent bonds.²⁸ The hydrogen bonds in complexes **3a** and **4a** are at the short end of this range and the distance increases with the size of the bridging group (Table 2) suggesting some limited flexibility in the cleft and, possibly, that the nitrate ion is a tight fit.

The persistence of the saddle conformation with different M(II) ions, coordination geometries, bridging species and exogenous ligands supports the suggestion of strong hydrogen bonding. Detailed NMR studies of the dizinc complex **2** suggest that the saddle conformation persists in solution. The ¹H NMR spectrum is relatively simple and was fully assigned with the help of COSY and NOE studies. It is notable that each methylene group shows two different proton environments consistent with the approximate *mm* symmetry of the $[\text{Zn}_2(\text{H}_4\text{L})\text{Cl}]^+$ cation (Fig. 1). There are no indications of fluxionality in the spectrum and this pattern is not significantly changed on heating to 60°.

Formation of the hyperbolic paraboloid core requires the presence of both the methylenediphenol groups and bound M(II)

ions to promote monodeprotonation and formation of the O–H–O links. The nature of the diamine used in formation of the macrocycle is less important, provided it can supply two donors in *cis* geometry at each metal ion. In the present case the pendant alcohol groups play no part in defining the geometry of the complexes (although they are involved in intermolecular hydrogen bonding). It should therefore be possible to vary the nature of the diamine without altering the core structure of the complex; hence it may be possible to build specific properties into the sides of the guest-binding cleft in order to promote reactivity at the dinuclear site. The dependence of the structure on the oxidation state of the coordinated metal ion also suggests that the 2,2'-methylenediphenol unit could be used as the basis of a two-way conformational switch. Formation or opening of the cleft could be driven by redox changes at the metal ion or by pH changes.

Finally, it should be pointed out that strong hydrogen bonding is not the only way of enforcing the hyperbolic paraboloid conformation. We have previously reported that it is possible to replace the pair of protons in the methylenediphenol groups with a copper(II) ion coordinated to all four phenolate donors, again with little change to the overall structure of the complex.¹⁵

Conclusions

The conformations of dinuclear complexes of H_6L are controlled by the protonation level of the methylenediphenol units. The protonation level depends on the oxidation state of the metal ions and, in di-M(II) complexes strong O–H–O interactions hold the macrocycle in a saddle-shaped conformation incorporating a site for exogenous ligands to bridge the two metal ions. Formally this sequence is akin to a cascade process;^{30,31} the ligand binds two M(II) ions, this causes monodeprotonation of the methylenediphenol groups and consequent assembly of a cleft incorporating a binding site for anions or neutral molecules.

Experimental

Synthesis

2,2'-Dihydroxy-5,5'-di-*tert*-butyl-3,3'-methanediyl dibenzaldehyde (dhtmb). The precursor 2,2'-dihydroxy-5,5'-di-*tert*-butyl-3,3'-methanediylalcohol was prepared from 4-*tert*-butylphenol as a white crystalline solid following the literature procedure¹⁹ with some minor modifications. The alcohol groups were oxidized to aldehyde by MnO_2 oxidation after the phenol groups had been protected using allyl bromide. The allyl groups were then removed using 10% Pd on charcoal to yield 2,2'-dihydroxy-5,5'-di-*tert*-butyl-3,3'-methanediyl dibenzaldehyde (dhtmb) in 40% yield for the three step process.^{14,20} Found: C 74.51, H 7.86. Calc. for $C_{23}H_{28}O_4$: C 74.97, H 7.66%. IR (KBr, cm^{-1}): 1658 ($\nu_{C=O}$), 1270 (s, ν_{Ar-OH}), 1216 (s). ¹H NMR ($CDCl_3$, 400 MHz) ppm: 11.19 [s, 2H, Ar–OH], 9.86 [s, 2H, CHO], 7.64 [d, 2H, ArH], 7.87 [d, 2H, ArH], 4.03 [s, 2H, Ar–CH₂–Ar], 1.29 [s, 18H, C(CH₃)₃].

The complexes were all prepared by template synthesis in ethanol. In a typical preparation one equivalent of the appropriate metal salt was dissolved in hot, dry ethanol along with one equivalent of dhtmb and the solution brought to reflux. One equivalent of 1,2-diaminopropan-2-ol in ethanol was added and refluxing continued for 2 h. The products were generally obtained on cooling the solution and reducing the volume. Details for each of the complexes are available in the electronic supplementary data.

[Cu₂(H₄L)Cl]Cl·2MeOH (1). Found: C 58.43, H 6.56, N 5.08. Calc. for $C_{34}H_{74}Cl_2Cu_2N_4O_8$ (1): C 58.68, H 6.75, N 5.07%. IR (KBr, cm^{-1}): 3421 (s, br); 2954 (s); 1626 (s, $\nu_{C=N}$); 1560 (w, ν_{C-O}); 1474 (m); 1363 (m); 1221 (m).

Emerald green crystals of the solvate $[Cu_2(H_4L)Cl]Cl \cdot 1.6Et_2O \cdot EtOH$ (1a) were obtained by diethyl ether diffusion into the filtrate.

[Zn₂(H₄L)Cl]Cl·H₂O (2). Found: C 58.76, H 6.52, N 5.26. Calc. for $C_{52}H_{68}Cl_2N_4O_7Zn_2$ (2): C 58.76, H 6.45, N 5.27%. IR (KBr, cm^{-1}): 3422 (s, br); 2963 (s); 1638 (s, $\nu_{C=N}$); 1553 (w, ν_{C-O}); 1479 (m); 1364 (m); 1220 (m). ¹H NMR ($CDCl_3$, 400 MHz) ppm: 8.10 [s, 4H, N=CH], 7.37 [d, 4H, ArH], 7.05 [d, 4H, ArH], 4.75 [d, 2H, Ar–CH₂–Ar], 4.51 [d, 4H, NCH₂], 4.25 [s (br), 2H, CHOH], 3.75 [dd, 4H, NCH₂], 3.55 [d, 2H, NCH₂], 1.28 [s, 36H, C(CH₃)₃]. ¹³C NMR ($CDCl_3$, 400 MHz) ppm: 171.4 [C=N], 157.1 [Ar–OH], 141.6 [Ar–Bu], 132.3 [C(Ar)H], 132.1 [Ar–C=N], 129.7 [C(Ar)H], 119.2 [Ar–CH₂–Ar], 68.2 [NCH₂], 67.9 [CH(OH)], 33.9 [Ar–CH₂–Ar], 31.3 [C(CH₃)₃], 31.0 [C(CH₃)₃].

The complex was crystallised from ethanol solution by slow diffusion of diethyl ether, yielding pale yellow crystals of $[Zn_2(H_4L)Cl]Cl \cdot Et_2O \cdot 0.5EtOH \cdot 0.55H_2O$ (2a) after a few days.

[Ni₂(H₄L)Cl]Cl·4H₂O (3). Found: C 56.57, H 6.50, N 4.70. Calc. for $C_{52}H_{74}Cl_2N_4O_{10}Ni_2$ (3): C 56.60, H 6.76, N 5.08%. IR (KBr, cm^{-1}): 3383 (s, br); 2956 (s); 1634 (s, $\nu_{C=N}$); 1551 (w, ν_{C-O}); 1476 (m); 1364 (m); 1223 (m).

[Co₂(H₄L)(H₂O)₃](ClO₄)₂·2H₂O (4). Found: C 50.01, H 5.63, N 4.29. Calc. for $C_{52}H_{76}Cl_2Co_2N_4O_{19}$ (4): C 49.96, H 6.13, N 4.48%. IR (KBr, cm^{-1}): 3423 (s, br); 2958 (s); 1630 (s, $\nu_{C=N}$); 1560 (w, ν_{C-O}); 1476 (m); 1436 (m); 1365 (m); 1223 (m); 1134 (s, $\nu_3(ClO_4^-)$); 1117 (s, $\nu_3(ClO_4^-)$); 1088 (s, $\nu_3(ClO_4^-)$); 626 (m, $\nu_4(ClO_4^-)$). Yellow crystals of $[Co_2(H_4L)(H_2O)(EtOH)_2](ClO_4)_2 \cdot 4EtOH$ (4a) were isolated by slow evaporation of an ethanol solution of the compound.

[Ni₂(H₄L)(H₂O)](ClO₄)₂·3H₂O (5). Found: C 51.09, H 6.39, N 4.26. Calc. for $C_{52}H_{72}Cl_2N_4Ni_2O_{17}$ (5): C 50.71, H 6.06, N 4.55%. IR (KBr, cm^{-1}): 3421 (s, br); 2959 (s); 1635 (s, $\nu_{C=N}$); 1561 (w, ν_{C-O}); 1476 (m); 1439 (m); 1365 (m); 1226 (m); 1107 (s, $\nu_3(ClO_4^-)$); 624 (m, $\nu_4(ClO_4^-)$). Pale green crystals of $[Ni_2(H_4L)(H_2O)(EtOH)_2](ClO_4)_2 \cdot 4EtOH$ (5a) were obtained directly from the reaction solution.

[Ni₂(H₄L)(NO₃)(H₂O)₂](NO₃)·H₂O (6). Found: C 55.10, H 6.20, N 7.12. Calc. for $C_{52}H_{76}N_6Ni_2O_{15}$ (6): C 54.86, H 6.37, N 7.38. IR (KBr, cm^{-1}): 3418 (ms); 2958 (s); 1634 (s, $\nu_{C=N}$); 1560 (w, ν_{C-O}); 1475 (m); 1384 (s, $\nu_3(NO_3^-)$); 1223 (m). Green crystals of $[Ni_2(H_4L)(NO_3)(dmf)_2](NO_3) \cdot 2dmf \cdot H_2O$ (6a) were obtained by slow evaporation of a dmf solution of $Ni_2(H_4L)(NO_3)_2(H_2O)_3$: dmf molecules replaced the coordinated water molecules.

[Zn₂(H₄L)(NO₃)(H₂O)₂](NO₃)·3H₂O (7). Found: C 54.01, H 6.19, N 7.87. Calc. for $C_{52}H_{72}N_6Zn_2O_{15}$ (7): C 54.21, H 6.30, N 7.29%. IR (KBr, cm^{-1}): 3426 (ms); 2957 (s); 1637 (s, $\nu_{C=N}$); 1559 (w, ν_{C-O}); 1475 (m); 1384 (s, $\nu_3(NO_3^-)$); 1221 (m). Pale yellow crystals of $[Zn_2(H_4L)(NO_3)(EtOH)]NO_3$ (7a) suitable for X-ray crystallography were obtained after a week.

[Mn₂(H₂L)(Cl)₂(EtOH)₂]·6H₂O (8). Found: C 54.99, H 7.39, N 4.94. Calc. for $C_{56}H_{88}Cl_2Mn_2N_4O_{14}$ (8): C 55.03, H 7.26, N 4.59%. IR (KBr, cm^{-1}): 3422 (s, br); 2958 (m); 1618 (s, $\nu_{C=N}$); 1550 (m, ν_{C-O}); 1439 (m); 1363 (w); 1309 (w); 1267 (m). Dark brown crystals of $[Mn_2(H_2L)(Cl)_2(dmf)(dmsO)] \cdot 1.5dmf \cdot 0.3Et_2O$ (8a) were obtained by slow diffusion of diethyl ether into a solution of 8 in dmf–dmsO.

X-Ray crystallography

Each data set was collected using a Bruker Smart 1000 CCD diffractometer. The structures were solved using direct methods and refined on F^2 using all the data.³² Data collection and refinement parameters are summarised in Table 3. Except as specified below, all non-hydrogen atoms were refined with anisotropic atomic displacement parameters. Hydrogen atoms bonded to carbon were inserted at calculated positions using a riding model and other hydrogen atoms were treated as described

Table 3 X-Ray data for the complexes

Complex	1a	2a	4a	5a	6a	7a	8a
Empirical formula	$[\text{Cu}_2(\text{H}_4\text{L})\text{Cl}]\text{Cl}\cdot 1.6\text{Et}_2\text{O}\cdot \text{EtOH}$	$[\text{Zn}_2(\text{H}_4\text{L})\text{Cl}]\text{Cl}\cdot \text{Et}_2\text{O}\cdot 0.5\text{EtOH}\cdot 0.55\text{H}_2\text{O}$	$[\text{Co}_2(\text{H}_4\text{L})(\text{H}_2\text{O})(\text{EtOH})_2](\text{ClO}_4)_2\cdot 4\text{EtOH}$	$[\text{Ni}_2(\text{H}_4\text{L})(\text{H}_2\text{O})(\text{EtOH})_2](\text{ClO}_4)_2\cdot 4\text{EtOH}$	$[\text{Ni}_2(\text{H}_4\text{L})(\text{NO}_3)(\text{dmf})(\text{dmso})]\cdot 1.5\text{dmf}\cdot 0.3\text{Et}_2\text{O}$	$[\text{Zn}_2(\text{H}_4\text{L})(\text{NO}_3)(\text{EtOH})\text{NO}_3]$	$[\text{Mn}_2(\text{H}_2\text{L})(\text{Cl})_2(\text{dmf})(\text{dmsO})]\cdot 1.5\text{dmf}\cdot 0.3\text{Et}_2\text{O}$
<i>M</i>	$\text{C}_{60.4}\text{H}_{88}\text{Cl}_3\text{Cu}_2\text{N}_4\text{O}_{8.6}$	$\text{C}_{57}\text{H}_{80.10}\text{ClN}_4\text{O}_{8.05}\text{Zn}_2$	$\text{C}_{64}\text{H}_{104}\text{Cl}_2\text{Co}_2\text{N}_4\text{O}_{21}$	$\text{C}_{64}\text{H}_{104}\text{Cl}_2\text{Ni}_2\text{N}_4\text{O}_{21}$	$\text{C}_{64}\text{H}_{60}\text{N}_{10}\text{Ni}_2\text{O}_{17}$	$\text{C}_{34}\text{H}_{72}\text{N}_4\text{O}_{13}\text{Zn}_2$	$\text{C}_{62.7}\text{H}_{90.5}\text{Cl}_2\text{Mn}_2\text{N}_6\text{O}_{9.8}\text{S}$
<i>T/K</i>	1205.73	1151.79	1454.27	1453.83	1388.88	1148.42	1304.96
<i>λ/Å</i>	0.71073	0.71073	0.71073	0.71073	0.71073	0.71073	0.71073
Crystal system	Triclinic	Triclinic	Orthorhombic	Orthorhombic	Monoclinic	Tetragonal	Monoclinic
Space group	$P\bar{1}$	$P\bar{1}$	$Pnma$	$Pnma$	$P2_1/c$	$I4_1/a$	$P2_1/c$
<i>a/Å</i>	13.707(3)	13.8372(7)	27.99433(17)	27.9805(12)	13.3462(5)	41.2744(13)	11.8935(8)
<i>b/Å</i>	14.568(3)	14.7550(7)	13.7494(8)	13.7050(6)	31.9837(13)	41.2744(13)	19.5914(13)
<i>c/Å</i>	16.827(4)	16.8022(8)	18.8620(11)	18.8743(8)	16.4255(6)	13.2831(6)	32.009(2)
<i>α/°</i>	103.472(3)	103.488(1)	90	90	90	90	90
<i>β/°</i>	95.935(3)	95.663(1)	90	90	90	90	100.683(1)
<i>γ/°</i>	93.429(3)	93.030(1)	90	90	90	90	90
<i>V/Å³</i>	3237.9(12)	3309.4(3)	7246.8(7)	7237.8(5)	6912.9(5)	22628.8(14)	7329.3(9)
<i>Z</i>	2	2	4	4	4	16	4
<i>D_c/Mg m⁻³</i>	1.237	1.156	1.333	1.334	1.334	1.348	1.183
Ref. collected	22822	23643	67304	50518	50389	80813	51860
Ind. refl. [<i>R</i> _{int}]	11279 [0.0455]	11600 [0.0167]	6669 [0.0937]	6664 [0.0234]	12167 [0.0558]	9961 [0.0466]	12907 [0.0486]
<i>R</i> ₁ , <i>wR</i> ₂ [<i>I</i> ≥ 2σ(<i>I</i>)]	0.0579, 0.1384	0.0722, 0.2137	0.0992, 0.2476	0.0764, 0.1899	0.0627, 0.1767	0.0510, 0.1430	0.0658, 0.1874
<i>R</i> ₁ , <i>wR</i> ₂ (all data)	0.1074, 0.1554	0.0827, 0.2262	0.1362, 0.2786	0.0840, 0.1949	0.0902, 0.1922	0.0686, 0.1521	0.0925, 0.2055

below for the individual structures. The crystals obtained were generally weakly-diffracting, having disordered and partial-occupancy solvate molecules in the lattice.

[Cu₂(H₄L)Cl]Cl·1.6Et₂O·EtOH (1a). The structure of this complex was reported earlier (CCDC reference number 190246).¹⁵ Data collection and refinement parameters are included in Table 3 for comparison.

[Zn₂(H₄L)Cl]Cl·Et₂O·0.5EtOH·0.55H₂O (2a). This complex is isomorphous with the copper analog 1a. The detailed structure differs in the occupancy of the solvate sites and in the disorder at the zinc sites discussed above. One disordered *tert*-butylphenol group was refined with 60 : 40 occupancy of two positions, and a second with 85 : 15 occupancy; one of the pendant alcohols showed 80 : 20 disorder over two positions; the ethanol solvate was modeled with partial (25 : 25) occupancy of two overlapping positions and the 25% occupancy carbon atoms were refined isotropically. The diethyl ether solvate molecules were each refined with 50% occupancy. No hydrogen atoms bonded to oxygen were located or included in the model.

[Co₂(H₄L)(H₂O)(EtOH)₂](ClO₄)₂·4EtOH (4a) and [Ni₂(H₄L)(H₂O)(EtOH)₂](ClO₄)₂·4EtOH (5a). The crystals are isomorphous, in each case the pendant alcohol group of the macrocycle is disordered 75 : 25 over two positions. The cations lie on mirror planes, as do the perchlorate anions, one of which is disordered (modeled as 45 : 5% over two sites on the mirror plane), and the uncoordinated ethanol solvate molecules. Hydrogen atoms bonded to oxygen atoms were located from difference maps and not further refined. The quality of the refinements was not improved by reducing the symmetry.

[Ni₂(H₄L)(NO₃)(dmf)₂]NO₃·2dmf·H₂O (6a). One of the coordinated dmf molecules is disordered, and was refined with 70 : 30 occupancy of two overlapping positions (both coordinated). There was one non-coordinated and ordered dmf solvate in the lattice but the remaining solvent was too disordered for individual atoms to be resolved; it was modeled as a diffuse contribution using the PLATON SQUEEZE procedure³³ within the WINGX package.³⁴ The electron density and void volume match one dmf and one water molecule per asymmetric unit and these were included in the formula. The hydrogen atoms bonded to the methylenediphenol units were located and not further refined; those bonded to the pendant alcohol groups were not located. One of the alcohol oxygen atoms is disordered with 50 : 50 occupancy of two equivalent sites.

[Zn₂(H₄L)(NO₃)(EtOH)]NO₃ (7a). The coordinated nitrate and one pendant alcohol are both disordered and were modelled with 60 : 40 occupancy of two related positions. Hydrogen atoms bonded to oxygen were all located and not further refined except for that bound to the disordered alcohol, which was not included in the refinement.

[Mn₂(H₂L)(Cl)₂(dmf)(dmsO)]·1.5dmf·0.3Et₂O (8a). In addition to the coordinated dmf and dmsO molecules, the lattice contained a partial-occupancy ether molecule, refined isotropically with 30% occupancy, one disordered dmf molecule, modeled with 50% occupancy of each of two overlapping sites and a further 50% occupancy dmf molecule. One of the pendant alcohol groups of the macrocycle was disordered and refined with 50% occupancy of two related positions and one of the *tert*-butyl groups was modeled with 60 : 40 occupancy of two positions. The hydrogen atoms of the pendant alcohols were not located or included in the model.

CCDC reference numbers 249422–249427.

See <http://www.rsc.org/suppdata/dt/b4/b413639j/> for crystallographic data in CIF or other electronic format.

Acknowledgements

We are grateful to the EPSRC Chemical Database Service at Daresbury for access to the CSD and to the EPSRC Mass Spectrometry Service, University of Swansea, for FAB (LSIMS) and ESI-MS data. We thank Dr M. Edgar, Loughborough University for assistance with the NMR studies.

References

- R. C. Long and D. N. Hendrickson, *J. Am. Chem. Soc.*, 1983, **105**, 1513.
- H. Okawa, J. Nishio, M. Ohba, M. Tadokoro, N. Matsumoto, M. Koikawa, S. Kida and D. E. Fenton, *Inorg. Chem.*, 1993, **32**, 2949.
- M. Yonemura, N. Usuki, Y. Nakamura, M. Ohba and H. Okawa, *J. Chem. Soc., Dalton Trans.*, 2000, 3624.
- A. Atkins, D. Black, A. J. Blake, A. Marin-Becerra, S. Parsons, L. Ruiz-Ramirez and M. Schroder, *Chem. Commun.*, 1996, 457.
- A. Hori, M. Yonemura, M. Ohba and H. Okawa, *Bull. Chem. Soc. Jpn.*, 2001, **74**, 495.
- M. J. Grannas, B. F. Hoskins and R. Robson, *Inorg. Chem.*, 1994, **33**, 1071.
- K. K. Nanda, S. Mohanta, U. Florke, S. K. Dutta and K. Nag, *J. Chem. Soc., Dalton Trans.*, 1995, 3831.
- V. McKee and S. S. Tandon, *J. Chem. Soc., Dalton Trans.*, 1991, 221.
- J. McCrea, V. McKee, T. Metcalfe, S. S. Tandon and J. Wikaira, *Inorg. Chim. Acta*, 2000, **297**, 220.
- D. C. Gutsche, *Calixarenes revisited*, ed. J. F. Stoddart, The Royal Society of Chemistry, Cambridge, 1998.
- A. J. Edwards, B. F. Hoskins, E. H. Kechab, A. Markiewicz, K. S. Murray and R. Robson, *Inorg. Chem.*, 1992, **31**, 3585.
- A. J. Edwards, B. F. Hoskins, R. Robson, J. C. Wilson, B. Moubaraki and K. S. Murray, *J. Chem. Soc., Dalton Trans.*, 1994, 1837.
- M. Bell, A. J. Edwards, B. F. Hoskins, E. H. Kachab and R. Robson, *J. Am. Chem. Soc.*, 1989, **111**, 3603.
- S. Goetz, PhD Thesis, Loughborough University, 2002.
- J. Barreira Fontecha, S. Goetz and V. McKee, *Angew. Chem., Int. Ed.*, 2002, **41**, 4554.
- H. Shimakoshi, H. Takemoto, I. Aritome and Y. Hisaeda, *Tetrahedron Lett.*, 2002, **43**, 4809.
- B. Masci, *Tetrahedron*, 2001, **57**, 2841.
- V. Böhmer, *Angew. Chem., Int. Ed. Engl.*, 1995, **34**, 713.
- B. Dhawan and C. D. Gutsche, *J. Org. Chem.*, 1983, **48**, 1536.
- J. Barreira Fontecha, S. Goetz and V. McKee, *Acta Crystallogr., Sect. C*, 2004, **60**, o776.
- F. H. Allen, *Acta Crystallogr., Sect. B*, 2002, **58**, 380.
- D. A. Fletcher, R. F. McMeeking and D. Parkin, *J. Chem. Inf. Comput. Sci.*, 1996, **36**, 746.
- D. Lee, P.-L. Hung, B. Springler and S. J. Lippard, *Inorg. Chem.*, 2002, **41**, 521, and references therein.
- D. Volkmer, B. Hommerich, K. Griesar, W. Haase and B. Krebs, *Inorg. Chem.*, 1996, **35**, 3792.
- K. K. Nanda, K. Venkatsubramanian, D. Majumdar and K. Nag, *Inorg. Chem.*, 1994, **33**, 1581.
- C. D. Gutsche, *Calixarenes*, Royal Society of Chemistry, Cambridge, 1989.
- N. A. Law, T. E. Machonkin, J. P. McGorman, E. J. Larson, J. W. Kampf and V. L. Pecorraro, *J. Chem. Soc., Chem. Commun.*, 1995, 2015.
- G. Gilli and P. Gilli, *J. Mol. Struct.*, 2000, **552**, 1.
- C. Giacobozzo, H. L. Monaco, G. Artioli, D. Viterbo, G. Ferraris, G. Gilli, G. Zanotti and M. Catti, *Fundamentals of Crystallography*, OUP, Oxford, 2002.
- J.-M. Lehn, *Science*, 1985, **227**, 849.
- J.-M. Lehn, *Pure Appl Chem.*, 1980, **52**, 2441.
- G. M. Sheldrick, *SHELXTL version 6.12*, Bruker-AXS, Madison WI, 2001.
- P. v. d. Sluis and A. L. Spek, *Acta Crystallogr., Sect. A*, 1990, **46**, 194.
- L. J. Farrugia, *J. Appl. Crystallogr.*, 1999, 837.